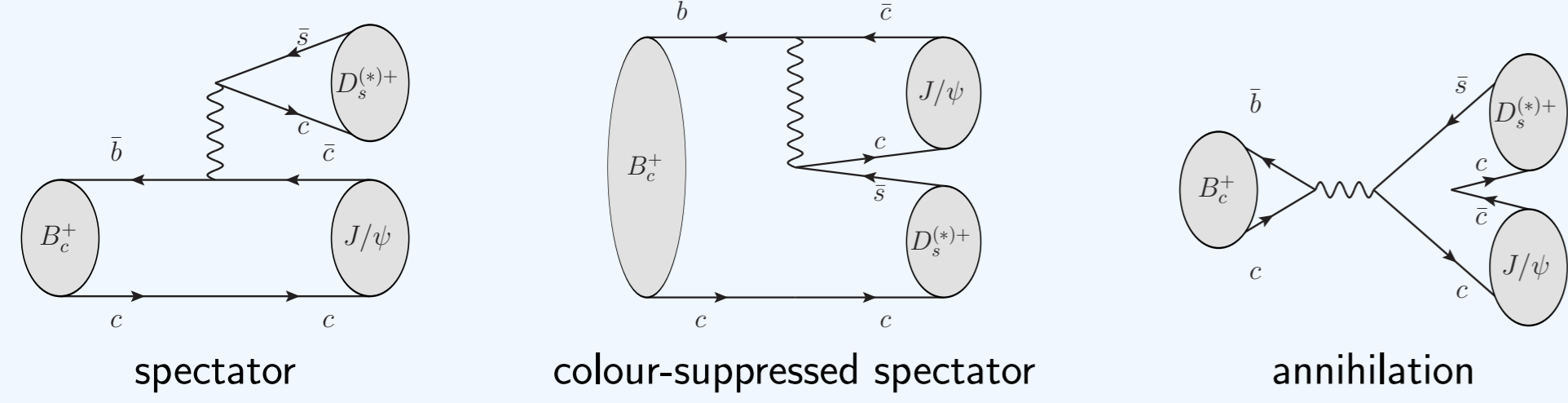


Study of $B_c^+ \rightarrow J/\psi D_s^+$ and $B_c^+ \rightarrow J/\psi D_s^{*+}$ decays in pp collisions at $\sqrt{s} = 13$ TeV with the ATLAS detector

1. Introduction

The B_c^+ meson is the only known weakly decaying particle consisted of two heavy quarks. It affects theoretical calculations of its decay properties. Various model predictions are available.

Leading Feynman diagrams for $B_c^+ \rightarrow J/\psi D_s^{(*)+}$ decays:



Unlike the other B mesons, the annihilation diagram is not CKM-suppressed

Measured quantities:

- Relative branching ratios

$$\mathcal{R}_{D_s^+/\pi^+} = \mathcal{B}(B_c^+ \rightarrow J/\psi D_s^+)/\mathcal{B}(B_c^+ \rightarrow J/\psi \pi^+)$$

$$\mathcal{R}_{D_s^{*+}/\pi^+} = \mathcal{B}(B_c^+ \rightarrow J/\psi D_s^{*+})/\mathcal{B}(B_c^+ \rightarrow J/\psi \pi^+)$$

$$\mathcal{R}_{D_s^{*+}/D_s^+} = \mathcal{B}(B_c^+ \rightarrow J/\psi D_s^{*+})/\mathcal{B}(B_c^+ \rightarrow J/\psi D_s^+)$$

- Transverse polarisation in $B_c^+ \rightarrow J/\psi D_s^{*+}$

4. Signal fits

An extended unbinned maximum-likelihood fit to the two-dimensional distribution of $m(J/\psi D_s^+)$ and $\cos\theta^l(\mu^+)$ is performed to extract the signal yields as well as the transverse polarization fraction in the $B_c^+ \rightarrow J/\psi D_s^{*+}$ decay. The helicity angle $\theta^l(\mu^+)$ is defined as the angle between μ^+ and D_s^+ candidate momenta in the rest frame of the muon pair.

Mass part

- $B_c^+ \rightarrow J/\psi D_s^+$ signal: modified Gaussian function

$$\text{Gauss}^{\text{mod}} \sim \exp\left(-\frac{x^{1+1/x/2}}{2}\right),$$

where $x = |m_0 - m|/\sigma$; width σ is fixed to MC simulation

- $B_c^+ \rightarrow J/\psi D_s^{*+}$ signals: sum of two templates for A_{00} and $A_{\pm\pm}$ contributions extracted from simulation with kernel estimate; fraction $f_{\pm\pm}$ is free parameter

- Background: exponential function

- Dataset 1:** candidates in the events collected by the standard dimuon or three-muon triggers – can be safely used to measure $R_{D_s^+/\pi^+}$, $R_{D_s^{*+}/\pi^+}$.
- Dataset 2:** candidates collected only by the dedicated $b\bar{b} \rightarrow \mu^+\mu^-\phi$ triggers – improve sensitivity to $R_{D_s^{*+}/D_s^+}$, $\Gamma_{\pm\pm}/\Gamma$.

5. Normalisation using reference decay

Selection of the reference decay candidates is close to that of signal for better cancellation of uncertainties

Same cuts as in $B_c^+ \rightarrow J/\psi D_s^{(*)+}$:

- J/ψ candidate selection
- $p_T(B_c^+)$, $|\eta(B_c^+)|$ region, $L_{xy}(B_c^+)$

Further cuts

- $|d_0^{\text{PV}}(B_c^+)/\sigma_{d_0^{\text{PV}}}(B_c^+)| < 3$ and $|z_0^{\text{PV}}(B_c^+)/\sigma_{z_0^{\text{PV}}}(B_c^+)| < 3$
- $\chi^2/\text{n.d.f.}(B_c^+) < 1.8$, $p_T(\pi^+) > 3.5$ GeV
- Veto π^+ candidate tracks identified as *low- p_T* muons to suppress $B_c^+ \rightarrow J/\psi \mu^+ \nu_\mu X$

Ratios of branching fractions:

$$R_{D_s^{(*)+}/\pi^+} = \frac{N_{B_c^+ \rightarrow J/\psi D_s^{(*)+}}^{\text{DS1}}}{N_{B_c^+ \rightarrow J/\psi \pi^+}} \times \frac{\epsilon_{B_c^+ \rightarrow J/\psi \pi^+}}{\epsilon_{B_c^+ \rightarrow J/\psi D_s^{(*)+}}^{\text{DS1}}} \times \frac{1}{\mathcal{B}(D_s^+ \rightarrow \phi(K^+K^-)\pi^+)},$$

$$R_{D_s^{*+}/D_s^+} = \frac{N_{B_c^+ \rightarrow J/\psi D_s^{*+}}^{\text{DS1\&2}}}{N_{B_c^+ \rightarrow J/\psi D_s^+}^{\text{DS1\&2}}} \times \frac{\epsilon_{B_c^+ \rightarrow J/\psi D_s^+}^{\text{DS1\&2}}}{\epsilon_{B_c^+ \rightarrow J/\psi D_s^{*+}}^{\text{DS1\&2}}} = r_{D_s^{*+}/D_s^+} \times \frac{\epsilon_{B_c^+ \rightarrow J/\psi D_s^+}^{\text{DS1\&2}}}{\epsilon_{B_c^+ \rightarrow J/\psi D_s^{*+}}^{\text{DS1\&2}}},$$

$$\Gamma_{\pm\pm}/\Gamma = f_{\pm\pm} \times \frac{\epsilon_{B_c^+ \rightarrow J/\psi D_s^{*+}}^{\text{DS1\&2}}}{\epsilon_{B_c^+ \rightarrow J/\psi D_s^{*+}, A_{\pm\pm}}^{\text{DS1\&2}}}$$

- $\mathcal{B}_{D_s^+ \rightarrow \phi(K^+K^-)\pi^+}$ – kaon pair mass dependent value from CLEO measurement [1]
- The total efficiencies – from MC simulation

Mode	DS1 $\epsilon_{B_c^+ \rightarrow J/\psi X}^{\text{DS1}}$ [%]	DS1&2 $\epsilon_{B_c^+ \rightarrow J/\psi X}^{\text{DS1\&2}}$ [%]
$B_c^+ \rightarrow J/\psi D_s^+$	0.971 ± 0.012	1.163 ± 0.013
$B_c^+ \rightarrow J/\psi D_s^{*+}, A_{00}$	0.916 ± 0.012	1.088 ± 0.012
$B_c^+ \rightarrow J/\psi D_s^{*+}, A_{\pm\pm}$	0.868 ± 0.010	1.049 ± 0.011
$B_c^+ \rightarrow J/\psi \pi^+$	2.169 ± 0.018	–

- They are different for A_{00} and $A_{\pm\pm}$ components of $B_c^+ \rightarrow J/\psi D_s^{*+}$ due to slightly different kinematics

$$\epsilon_{B_c^+ \rightarrow J/\psi D_s^{*+}}^{\text{DS1\&2}} = \left(f_{\pm\pm}/\epsilon_{B_c^+ \rightarrow J/\psi D_s^{*+}, A_{\pm\pm}}^{\text{DS1\&2}} + (1 - f_{\pm\pm})/\epsilon_{B_c^+ \rightarrow J/\psi D_s^{*+}, A_{00}}^{\text{DS1\&2}} \right)^{-1}$$

2. Reconstruction and measurement strategy

Signal modes: $B_c^+ \rightarrow J/\psi D_s^+$ and $B_c^+ \rightarrow J/\psi D_s^{*+}$

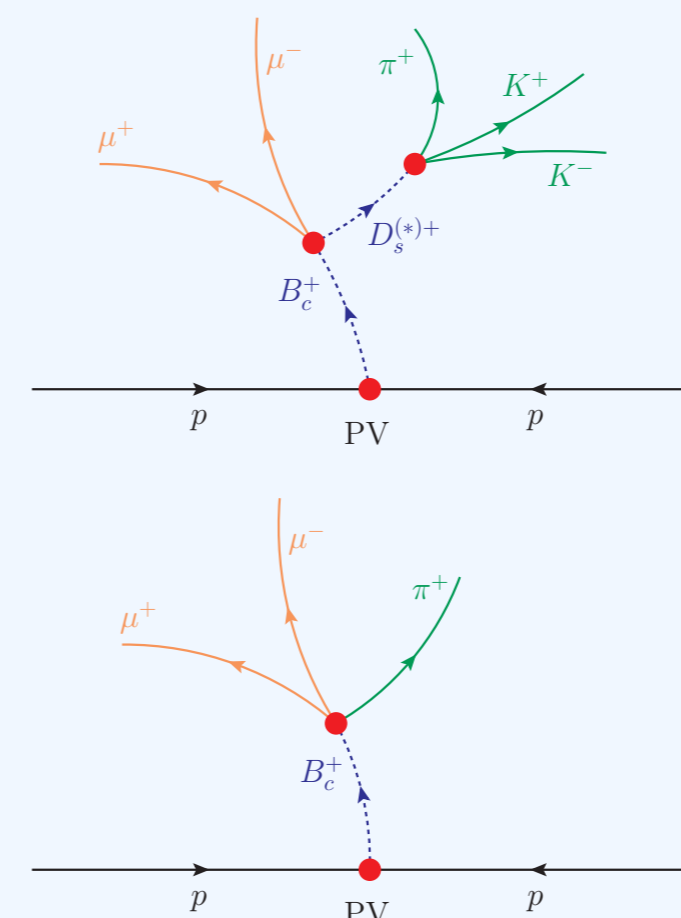
- Daughters are reconstructed via $J/\psi \rightarrow \mu^+ \mu^-$ and $D_s^+ \rightarrow \phi \pi^+$ with $\phi \rightarrow K^+ K^-$
- 2 distinct decay vertices of B_c^+ and D_s^+ decays
- Masses of J/ψ and D_s^+ candidates are constrained in the vertex fit to their nominal values
- D_s^{*+} decays into $D_s^+ \gamma$ or $D_s^+ \pi^0$ with the neutral particle escaping detection, i.e. incomplete reconstruction

Reference mode: $B_c^+ \rightarrow J/\psi \pi^+$

- One secondary vertex of B_c^+ decay; J/ψ candidate mass is constrained in the fit to the nominal value
- The mode provides large statistics and thus used for normalisation in the branching fractions measurement

Polarisation in $B_c^+ \rightarrow J/\psi D_s^{*+}$ decay

- Scalar B_c^+ decays into two vector particles \rightarrow three possible helicity amplitudes A_{00}, A_{++}, A_{--}
- Longitudinal A_{00} and transverse $A_{\pm\pm}$ components have different kinematics:
 - shape of $J/\psi D_s^+$ invariant mass and J/ψ helicity angle
- They can be distinguished in the fit to these variables



3. Event selection

Preselection

J/ψ candidates

The J/ψ candidates are built from pairs of oppositely charged muon candidates that are reconstructed using information from the MS and the ID. Muon candidates must satisfy the *Loose* identification working point

D_s^+ candidates

- $p_T(\text{trk}) > 1$ GeV, $|\eta(\text{trk})| < 2.5$
- $L_{xy}(D_s^+) > 0$ mm (w.r.t the B_c^+ vertex)
- $m(\phi) \pm 7$ MeV around nominal ϕ mass
- $1.93 \text{ GeV} < m(K^+ K^- \pi^+) < 2.01 \text{ GeV}$

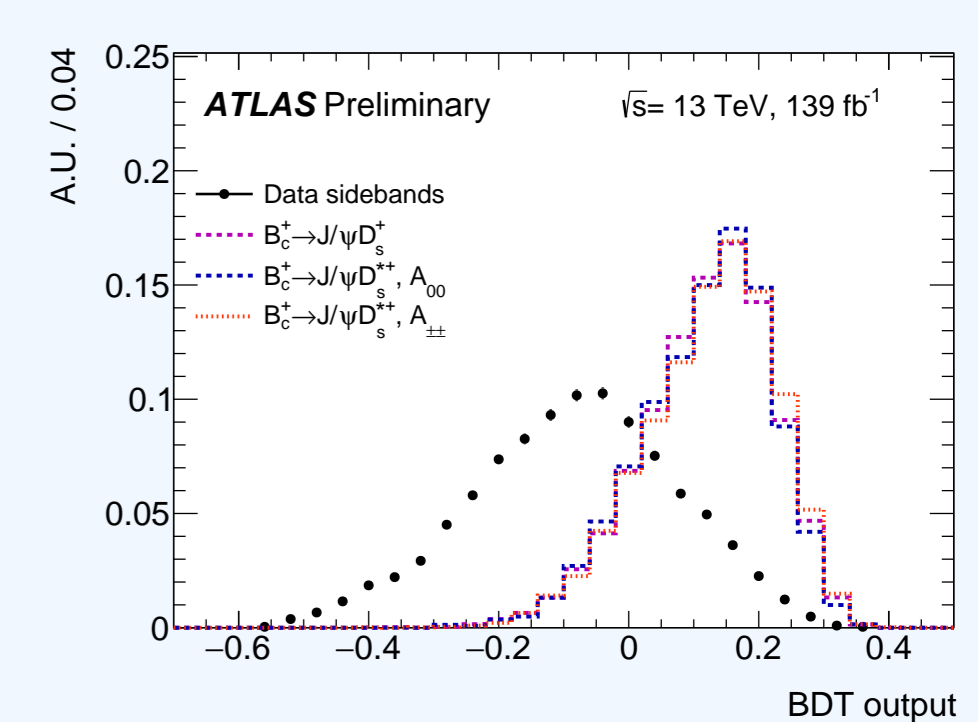
B_c^+ candidates

- $p_T(B_c^+) > 15$ GeV, $|\eta(B_c^+)| < 2.1$
- $|d_0^{\text{PV}}(B_c^+)/\sigma_{d_0^{\text{PV}}}(B_c^+)| < 5$ and $|z_0^{\text{PV}}(B_c^+)/\sigma_{z_0^{\text{PV}}}(B_c^+)| < 5$ w.r.t the PV
- Vertex $\chi^2/\text{n.d.f.} < 2$, $\text{n.d.f.} = 8$
- $L_{xy}(B_c^+) > 0.3$ mm, $L_{xy}(B_c^+) < 10$ mm
- Exclude $5.34 \text{ GeV} < m(J/\psi \phi) < 5.40 \text{ GeV}$ to suppress $B_s^0 \rightarrow J/\psi \phi$

To further suppress the combinatorial background, a multivariate classifier based on boosted decision trees (BDT) as implemented in the TMVA framework is employed.

BDT input variables

- $p_T(D_s^+)$, $L_{xy}(D_s^+)$
- $\cos\theta^*(\pi^+)$, $|\cos^3\theta^*(K^+)|$ (for D_s^+)
- $\cos\theta^*(D_s^+)$, $\cos\theta^*(\pi^+)$ (for B_c^+)



6. Systematics

Source	Uncertainty [%]			
	$R_{D_s^+/\pi^+}$	$R_{D_s^{*+}/\pi^+}$	$R_{D_s^{*+}/D_s^+}$	$\Gamma_{\pm\pm}/\Gamma$
Simulated $p_T(B_c^+)$ spectrum	1.5	1.9	0.4	0.1
Simulated $ \eta(B_c^+) $ spectrum	0.7	0.7	0.1	0.2
B_c^+ lifetime	0.1	< 0.1	–	–
D_s^+ lifetime	0.4	0.4	–	–
Tracking efficiency	1.0	1.0	< 0.1	< 0.1
Pile-up effects	1.0	1.0	–	–
$\chi^2/\text{n.d.f.}$ cut efficiency	3.2	3.2	–	–
Impact parameter cuts efficiency	0.2	0.2	–	–
BDT cut efficiency	1.3	1.3	–	–
Trigger efficiency	1.0	1.0	–	–
$B_c^+ \rightarrow J/\psi D_s^{(*)+}$ signal fit:				
D_s^+ signal mass modelling	1.8	0.5	1.3	0.8
D_s^{*+} signal mass modelling	0.6	1.2	1.7	2.7
signal angular modelling	0.4	< 0.1	0.4	0.6
background mass modelling	6.0	9.0	3.2	1.0
background angular modelling	0.9	1.3	2.1	2.4
$B_c^+ \rightarrow \mu^+ \mu^- \phi$ triggers	0.8	0.5	1.3	4.0
$B_c^+ \rightarrow J/\psi \pi^+$ signal fit:				
signal modelling	4.2	4.2	–	–
PRD/comb. background modelling	5.8	5.8	–	–
CKM-suppr. background modelling	1.0	1.0	–	–
MC statistics				
Total	10.7	12.6	5.0	5.8
$\mathcal{B}(D_s^+ \rightarrow \phi(K^+K^-)\pi^+)$	5.9	5.9	–	–

7. Results

Measured ratios of branching fractions:

$$\mathcal{R}_{D_s^+/\pi^+} = 2.76 \pm 0.33(\text{stat.}) \pm 0.29(\text{syst.}) \pm 0.16(\text{BF})$$

$$\mathcal{R}_{D_s^{*+}/\pi^+} = 5.33 \pm 0.61(\text{stat.}) \pm 0.67(\text{syst.}) \pm 0.32(\text{BF})$$

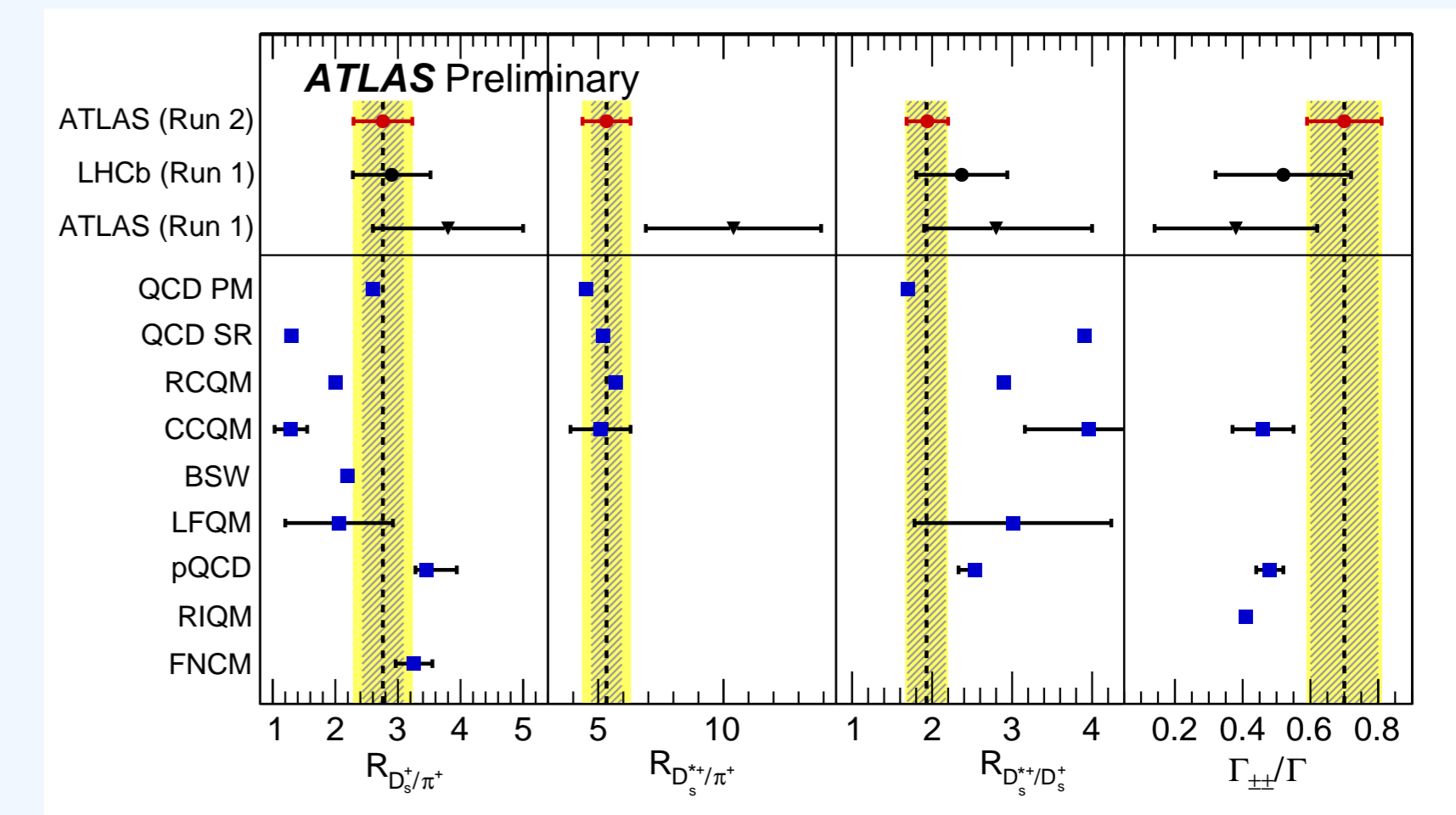
$$\mathcal{R}_{D_s^{*+}/D_s^+} = 1.93 \pm 0.24(\text{stat.}) \pm 0.1(\text{syst.})$$

(BF error corresponds to the knowledge of $\mathcal{B}_{D_s^+ \rightarrow \phi(K^+K^-)\pi^+}$)

Transverse polarisation fraction in $B_c^+ \rightarrow J/\psi D_s^{*+}$:

$$\Gamma_{\pm\pm}/\Gamma = 0.70 \pm 0.10(\text{stat.}) \pm 0.04(\text{syst.})$$

The measurements of $R_{D_s^+/\pi^+}$ and $R_{D_s^{*+}/D_s^+}$ agree with ATLAS Run 1 [2] and LHCb [3] results. The obtained value of the $R_{D_s^{*+}/\pi^+}$ is smaller and $\Gamma_{\pm\pm}/\Gamma$ is larger than the ATLAS Run 1 measurement, although in both cases the difference does not exceed 1.5 standard deviations taking the Run 1 uncertainty. All the ratios of branching fractions are well described by the QCD relativistic potential model predictions [4].



References

- CLEO Collaboration, *Absolute Measurement of Hadronic Branching Fractions of the D_s^+ Meson*, *Phys. Rev. Lett* **100** (2008) 161804, arXiv:0801.0680 [hep-ex].
- ATLAS Collaboration, *Study of the $B_c^+ \rightarrow J/\psi D_s^+$ and $B_c^+ \rightarrow J/\psi D_s^{*+}$ decays with the ATLAS detector*, *Eur. Phys. J. C* **76** (2016) no.1, 4, arXiv:1507.07099 [hep-ex].
- LHCb Collaboration, *Observation of $B_c^+ \rightarrow J/\psi D_s^+$ and $B_c^+ \rightarrow J/\psi D_s^{*+}$ decays*, *Phys. Rev. D* **87** (2013) 112012, arXiv:1304.4530 [hep-ex].
- P. Colangelo and F. De Fazio, *Using heavy quark spin symmetry in semileptonic B_c decays*, *Phys. Rev. D* **61** (2000), 034012, arXiv:hep-ph/9909423 [hep-ph].